



A dual response near-infrared fluorescent probe for hydrogen polysulfides and superoxide anion detection in cells and in vivo



Fabiao Yu, Min Gao, Meng Li, Lingxin Chen*

Key Laboratory of Coastal Environmental Processes and Ecological Remediation, The Research Centre for Coastal Environmental Engineering and Technology, Yantai Institute of Coastal Zone Research, Chinese Academy of Sciences, Yantai 264003, China

ARTICLE INFO

Article history:

Received 28 May 2015

Received in revised form

4 June 2015

Accepted 6 June 2015

Available online 10 June 2015

Keywords:

Fluorescent probe

Image analysis

Hydrogen polysulfides

Superoxide anion

Near-infrared

ABSTRACT

Intracellular reactive sulfur species play important roles in physiological and pathological processes. Emerging evidences suggest that sulfane sulfur instead of H₂S is the actual signaling molecule in these processes. Sulfane sulfur can be generated as a result of the reaction between O₂^{•-} and H₂S in mitochondria. Therefore, we develop a near-infrared mitochondria-targeting probe that allows multiresponse to O₂^{•-} and H₂S_n successively for investigating this biosynthetic reaction. The probe exhibits highly selective fluorescent response to O₂^{•-} and H₂S_n successively in presence of potential biological interferences. Fluorescent imaging studies and flow cytometry analysis of RAW264.7 cells elaborate that the probe can be used to reveal the continuous process of O₂^{•-} burst and H₂S_n production in situ and in real-time. The mitochondria isolation indicates that the probe can specifically localize in mitochondria. Finally, the fluorescent probe has been successfully applied to detect O₂^{•-} and H₂S_n in mice.

© 2015 Elsevier Ltd. All rights reserved.

1. Introduction

The intracellular reactive sulfur species is a general term for sulfur-containing biomolecules which assumes critical responsibilities for physiological and pathological processes in vivo [1–8]. Among those biomolecules, H₂S has been known as the third gas transmitter [9,10]. However, the existence of this gas in cells should be controlled closely, because the abnormal level of H₂S will cause potential adverse effects to mitochondrial respiration, and then many diseases may be induced [11,12]. Therefore, the sulfur-relevant cell signaling processes should depend on the rapid H₂S metabolism via biochemical pathways. It is reported that the endogenous H₂S metabolism can be balanced through oxygen-dependent sulfane sulfur production in mitochondria [13,14]. Sulfane sulfur are an uncharged form of sulfur (S⁰) with six valence electrons, which can be reversibly attached to proteins via covalent bond between S⁰ and other sulfur atoms [11,12,15]. They are mainly present in hydrogen polysulfides (H–S_n–SH, n ≥ 1), alkyl hydroper-sulfide (R–SSH), alkyl hydro-polysulfides (R–S_n–SH, n ≥ 1), alkyl polysulfides (R–S–S_n–S–R, n ≥ 1), and elemental sulfur (S₈). Compared with H₂S, sulfane sulfur exhibit low cytotoxicity in

biological systems. It is possible that H₂S produced by enzymes will be immediately converted into sulfane sulfur and stably stored in cells for the further signaling regulation [16]. Additionally, emerging evidences suggest that the actual signaling molecules in vivo are sulfane sulfur rather than H₂S [13–15]. However, the biosynthetic pathways and biofunctions of sulfane sulfur are still under investigation. Some recent examinations imply that sulfane sulfur can be derived from H₂S in presence of reactive oxygen species (ROS) [17–19]. As the base composition of sulfane sulfur, H₂S_n are involved in cytoprotective processes and redox signaling. Moreover, the species can be considered as the redox forms of H₂S [20,21].

Mitochondria are main production source of ROS. During the process of mitochondrial respiration, a small portion of oxygen (0.1%–4%) is always reduced to superoxide anion (O₂^{•-}) by electrons leak from respiratory chain. Subsequently, O₂^{•-} can be converted into other ROS enzymatically or non-enzymatically, which indicates that the concentration of O₂^{•-} can reflect the levels of other ROS [22]. In cells, the mitochondria fraction contains approximately 60% of bound sulfane sulfur [16]. We hypothesize that the mitochondria-targeting H₂S_n production may benefit from O₂^{•-}, although the real situation remains to be elucidated. In order to comprehend the production of H₂S_n in presence of O₂^{•-}, it is essential to develop new analytical methods for the direct detection of intracellular O₂^{•-}/H₂S_n in situ and in real-time.

* Corresponding author.

E-mail address: lxchen@yic.ac.cn (L. Chen).

The measurement of the intracellular concentrations of $O_2^{\cdot-}/H_2S_n$ under physiological and pathophysiological conditions suffers many challenges due to the lack of direct chemical tools. In biological system, $O_2^{\cdot-}$ features with some labile natures, such as low concentration, high reactivity, and short lifetime. What is more, the process of produce and transport H_2S_n by both inhibition and activation of enzymes always occur at a very low and narrow concentration range within a short time precisely [23]. The bio-systems which are thought to generate H_2S_n may successively produce H_2S through reduced reaction. The exogenous supplement of H_2S to a system can also be considered to add H_2S_n [15]. Given the reversible relationship between H_2S and H_2S_n , it seems that we cannot isolate H_2S_n from H_2S in assay system. Coupled with the participation of $O_2^{\cdot-}$, the redox signaling process requires an effective detection method. In comparison with other biological detection technologies, fluorescence bioimaging technology has become a powerful supporting tool for the detection of intracellular reactive species. This method offers several attractive advantages, such as high spatial and temporal resolution, less invasiveness, good sensitivity, excellent selectivity, and rapid response [1–8]. Although much progress had been made in the development of fluorescent probes for $O_2^{\cdot-}$ [1–6,24–27] and H_2S_n [28–32] detection separately, fluorescent probes for $O_2^{\cdot-}$ and H_2S_n successively detection are more desirable due to the redox signaling process between $O_2^{\cdot-}$ and H_2S_n is a complex redox process which involves various species at the same time in living cells. As far as the signaling process is concerned, a probe which can selectively respond to multi-species should be more appropriate for visualizing the redox process and should offer important future directions for biological events [33–47]. The signaling process may be examined by combination of two separate fluorescent probes, one is for $O_2^{\cdot-}$ and the other is for H_2S_n . However, this solving strategy often suffers from inaccurate calibration and circumvent complications including photobleaching rates of individual probes, uneven probe loading, nonhomogeneous distribution uncontrollable localization, larger invasive effects, metabolisms, and interference of spectral overlap [37,48]. All above influencing factors may limit the spatial dimensions for intracellular application and make the probe unsuitable for quantitative analysis [48]. In order to achieve better fluorescent imaging, the development of excellent fluorescent probes is urgently required. Compared with the single response probes, the multiresponse probes can effectively avoid the above mentioned influencing factors. Therefore, we strive to conceive and synthesize a multiresponse probe that can directly deliver sensitive and multi-channel fluorescence signals from a single dye for the detection of intracellular $O_2^{\cdot-}/H_2S_n$ level changes in situ and in real-time. Additionally, the long wavelength multiresponse probes which can emit in near-infrared (NIR) range are essential for in vivo imaging, because the NIR fluorescence can maximize the depth penetration and minimize the background autofluorescence signal.

Once capturing the key issues of our research, it is desirable to develop a NIR multiresponse probe for directly exploring the mitochondria-targeting H_2S_n production which benefits from $O_2^{\cdot-}$. Herein, we design and synthesize a multiresponse near-infrared fluorescent probe HCy-FN for the detection of $O_2^{\cdot-}$ and H_2S_n successively (Scheme 1). The probe is investigated to be selective for the detection of $O_2^{\cdot-}$ and H_2S_n with response time of 3 and 0.5 min, respectively. These features play a crucial role for rapid detection owing to the fast metabolism of $O_2^{\cdot-}$ and H_2S_n during redox signaling process. Fluorescence confocal microscopic images and flow cytometry analysis demonstrate that our probe can detect the mitochondrial $O_2^{\cdot-}$ and H_2S_n successively in RAW264.7 cells and in mice with dual channel response.

2. Materials and methods

2.1. Synthesis of probe

Scheme 2 outlined the synthetic procedures of the probe HCy-FN. Ketone cyanine 3 (Keto-Cy) was derivative from a near-infrared (NIR) heptamethine cyanine dye Cy.7.Cl [49]. After the acyl-chlorination, 2-fluoro-5-nitrobenzoic acid was converted to 2-fluoro-5-nitrobenzoyl chloride in hydrous CH_2Cl_2 at 25 °C. The solvent was evaporated immediately, and then Keto-Cy was added to continue alcoholysis. The reaction product was afforded as 2 (Cy-FN). The iminium cations of Cy-FN could be reduced with $NaBH_4$ to produce the final product 1 hydroCy-FN (HCy-FN) [50]. The synthetic details of these compounds were shown in the Supporting Information (SI).

2.2. Imagings in cells and mice

Mouse macrophage cell line (RAW264.7) was obtained from the Committee on Type Culture Collection of Chinese Academy of Sciences (Shanghai, China). RAW264.7 cells were grown in high glucose Dulbecco's Modified Eagle Medium (DMEM, 4.5 g of glucose/L) supplemented with 10% Fetal Bovine Serum (FBS). Cells were plated on 25-Petri dishes and allowed to adhere for 24 h before imaging. BALB/c mice were obtained from Binzhou Medical University. Mice were group-housed on a 12:12 light–dark cycle at 22 °C with free access to food and water. BALB/c mice (20–25 g) were selected and divided into different groups. Images were taken by Bruker In-vivo Imaging System.

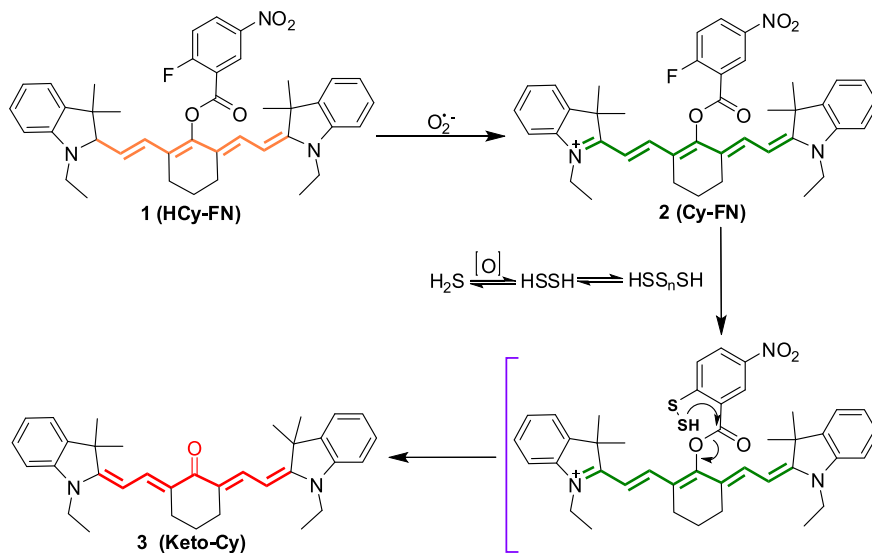
3. Results and discussion

3.1. Strategies for fluorescent probe

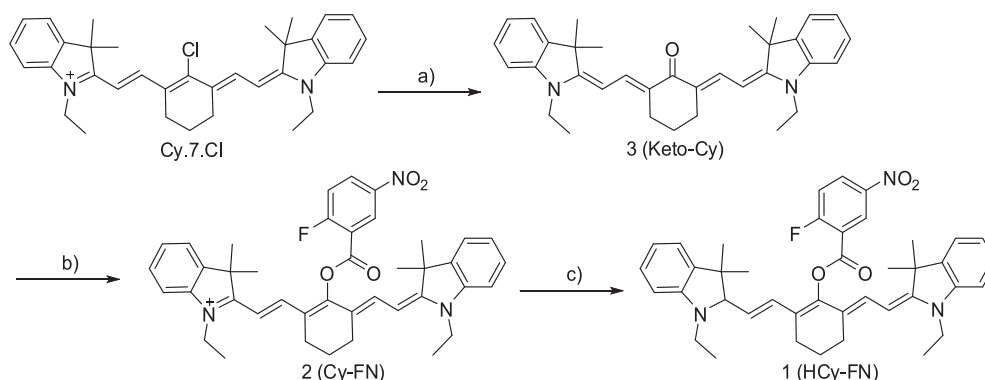
Our overall strategy for the imaging of $O_2^{\cdot-}/H_2S_n$ successively in live biological systems is inspired by exploiting two selective chemical reactions. One is hydrogen abstraction reaction for $O_2^{\cdot-}$ detection [27,51,52], the other is bis-electrophilic reaction for H_2S_n detection [7,8,28–32]. We choose near-infrared (NIR) heptamethine cyanine (Cy) as signal transducer because the iminium cations of this fluorophore platform can be reduced to hydrocyanine for the further $O_2^{\cdot-}$ detection. Furthermore, the absorption and emission of fluorophore which locate in the NIR region will be more suitable for the in vivo detection, because the NIR absorption and emission profiles can maximize tissue penetration while minimizing the absorbance of heme in hemoglobin and myoglobin, water, and lipids [53,54]. Next, we select nitro-activated fluorobenzoate as fluorescent modulator since the bis-electrophilic center existed in this group can be used for trapping H_2S_n , the direct redox form of H_2S , which may act as the initial reactive polysulfide species in cells [14,15,55,56]. Our design outline for intracellular $O_2^{\cdot-}/H_2S_n$ detection was illustrated in Scheme 1. The fluorescent probe HCy-FN functioned by modulating the polymethine π -electron system via conjugation [57,58] for $O_2^{\cdot-}$ detection and by the removal of certain trigger moiety, nitro-activated fluorobenzoate, for H_2S_n detection.

3.2. Fluorescence response to $O_2^{\cdot-}$ and H_2S_2

H_2S_n are composed of a series of hydrogen polysulfides species [20,21]. There exists a dynamic distribution of these hydrogen polysulfides species under certain pH condition (Scheme 1). Taking all these factors into account, we attempted to pick out hydrogen disulfide (H_2S_2) as the testing target since this simple hydrogen polysulfides undergone bis-electrophilic reaction more unambiguously.



Scheme 1. Proposed reaction mechanism for $O_2^{\cdot-}$ and H_2S_n detection.



Scheme 2. Strategy and synthesis routes for probe HCy-FN. Notes: (a) sodium acetate, anhydrous DMF, 80 °C 3 h, 85%; (b) 2-fluoro-5-nitrobenzoic acid, chloroglyoxylate, anhydrous CH_2Cl_2 , 25 °C 4 h; 2-fluoro-5-nitrobenzoyl chloride, anhydrous CH_2Cl_2 , 0 °C 1 h, then 25 °C 12 h, 50%; (c) methanol, $NaBH_4$ 1.5 eq., 0 °C 10 min, 80%. All above experiments were performed under Ar condition.

We checked the spectroscopic response of our probe under simulated physiological conditions (10 mM HEPES pH 7.4). The spectral properties of the compounds (**1–3**) were summarized in Table 1. As shown in Figs. S4–S10, our probe could detect the changes of the concentration of $O_2^{\cdot-}/H_2S_n$ under the given range, which revealed the ability of our probe for the selective and sensitive detection of $O_2^{\cdot-}/H_2S_n$ potentially in cells (see SI).

3.3. Monitoring H_2S_n formation between ROS and H_2S

Although the biosynthetic pathways of H_2S_n are far from abundantly clear, more and more research results suggest that they can be derived from H_2S in the presence of ROS [17–28]. Next, we discussed the capability of our probe HCy-FN for real-time detecting H_2S_n generation from the reaction between H_2S and ROS. The

fluorescence signal were recorded from channel 1: 794 nm ($\lambda_{ex} = 750$ nm) and channel 2: 625 nm ($\lambda_{ex} = 535$ nm) synergistically. As shown in Fig. 1, the addition of $O_2^{\cdot-}$ (50 μ M) into HCy-FN (5 μ M) solution triggered the fluorescent switch on efficaciously within 3 min (channel 1). The fluorescence of channel 2 showed no response. Then NaHS (50 μ M) was added, the fluorescence intensity of channel 1 decreased gradually and channel 2 gave some increase during 10 min. We attributed the fluorescence changes of channel 2 to the generation of H_2S_n from H_2S in presence of $O_2^{\cdot-}$. However, the chemical synthetic pathway is so slow that it may not consistent with the biofunction of H_2S_n because these reactive sulfur species only play their physiological roles under a narrow concentration within a short time. It is reported that glutathione peroxidase (GPx) can eliminate ROS through depleting reducing thiols, such as GSH and Cys. There are evidences suggest that GPx can also scavenge ROS by utilizing H_2S to produce H_2S_n [65–68]. Subsequently, we added GPx (500 U/L) as catalyst to accelerate the reaction rate. As expected, the channel 1 and channel 2 exhibited quick changes in fluorescence intensity upon the reaction of H_2S_n . The fluorescence intensity of channel 2 could reach saturation within 15 min, which indicated that H_2S_n might be produced by the enzymes involved reaction between $O_2^{\cdot-}$ and H_2S . These results demonstrated that our probe HCy-FN possessed the capability of

Table 1
Summary of spectral properties of compounds **1**, **2** and **3**.

	Absorption: λ_{max} (nm); ϵ ($cm^{-1} M^{-1}$)	Emission: λ_{max} (nm); ϕ
1 (HCy-FN)	Unavailable	Unavailable
2 (Cy-FN)	775; 1.1×10^5	794; 0.0203
3 (Keto-Cy)	535; 4.9×10^4	625; 0.361

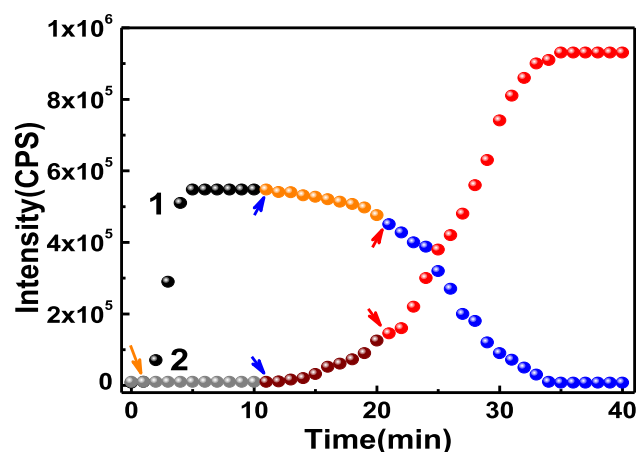


Fig. 1. Fluorescence response of Hcy-FN to H_2S_n which produced via $\text{O}_2^{\cdot-}$ reacting with H_2S . Hcy-FN ($5 \mu\text{M}$) reacts with $\text{O}_2^{\cdot-}$ ($50 \mu\text{M}$) for 10 min, next NaHS ($50 \mu\text{M}$) was added for another 15 min, and then added glutathione peroxidase (GPx, 500 U/L) for the last 10 min. Channel 1: $\lambda_{\text{ex}} = 750 \text{ nm}$ and $\lambda_{\text{em}} = 794 \text{ nm}$; Channel 2: $\lambda_{\text{ex}} = 535 \text{ nm}$ and $\lambda_{\text{em}} = 625 \text{ nm}$.

detection of $\text{O}_2^{\cdot-}$ and H_2S_n in situ by employing different emission channels.

Next we employed the probe Cy-FN to test other physiological relevant ROS and RNS in H_2S solution. After exposed $\cdot\text{OH}$, H_2O_2 , ONOO^- to H_2S in the presence of GPx, Cy-FN exhibited strong fluorescent increase (Fig. S11). Exceptionally, H_2S together with ClO^- afforded a strong response without GPx. We attributed the reason to the relative reactivities of one-electron oxidants which based on reduction potential. And those of two-electron oxidants were based on the reaction rates with antioxidants [63]. Therefore, ClO^- might occupy a faster reaction rate converting H_2S to H_2S_n in absence of GPx. Above all, we verified that GPx was involved in the reaction between ROS and H_2S as a catalyst.

3.4. Bioimaging of $\text{O}_2^{\cdot-}$ and H_2S_n in cells

Our probe Hcy-FN exhibited high properties of sensitivity and selectivity in solution, we next examined whether the probe could respond to $\text{O}_2^{\cdot-}$ and H_2S_n successively using dual collected channels of confocal fluorescence microscopy. The mouse macrophage cell line RAW264.7 was chosen as the bioassay model throughout the paper. RAW264.7 cells were loaded with $1 \mu\text{M}$ Hcy-FN for 15 min. After washed with RPMI-1640, the cells were treated with $\text{O}_2^{\cdot-}$ and NaHS (a normal H_2S donor, pre- H_2S_n source), and then for

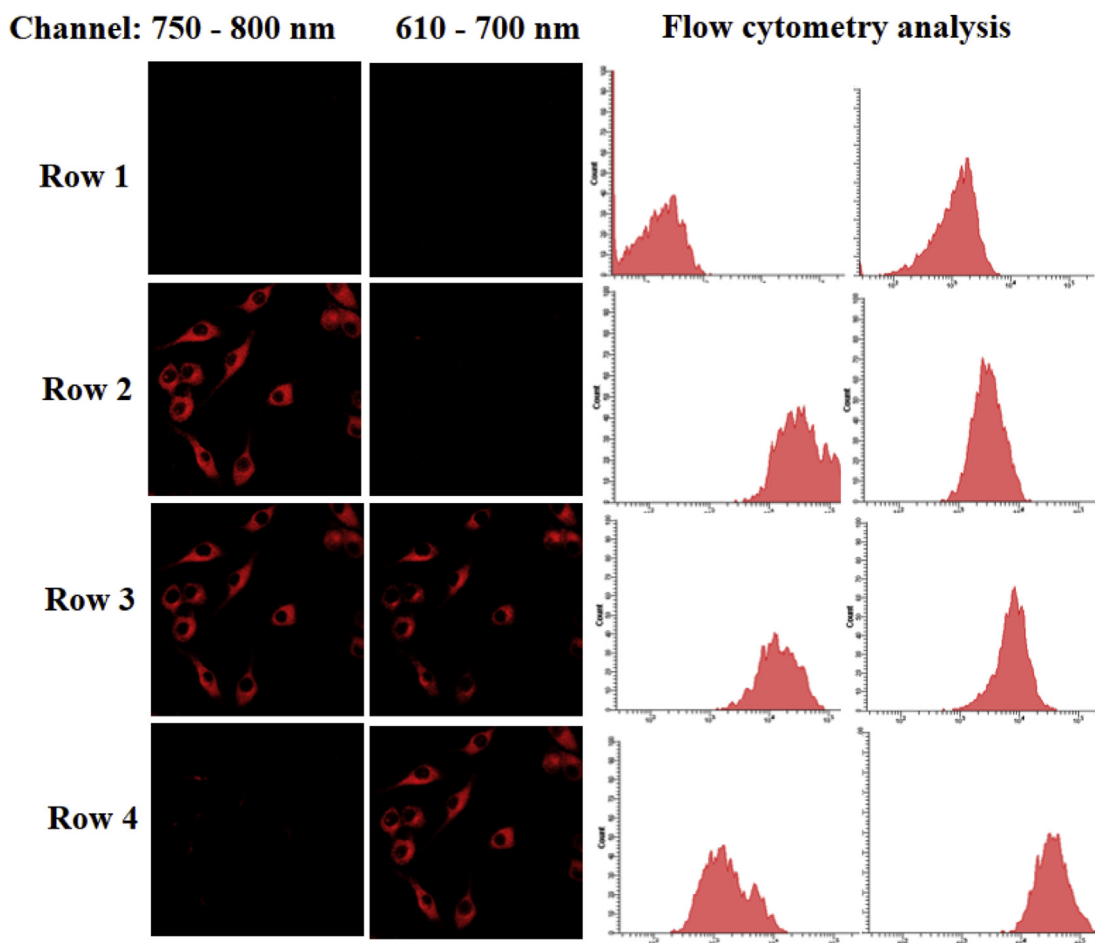


Fig. 2. Fluorescence confocal microscopic images of RAW264.7 cells exposed to $\text{O}_2^{\cdot-}$ and NaHS (pre- H_2S_n source) showing the fluorescent response as a function of time after incubation with probe Hcy-FN. RAW264.7 cells were incubated with $1 \mu\text{M}$ Hcy-FN at 37°C for 15 min. The images were obtained at time points consisting of 5, 10 and 20 min after the sequential addition of $\text{O}_2^{\cdot-}$ and NaHS. Representative flow cytometric analysis for the cells shown at left. Fluorescence bioimaging collection windows: from 760 to 850 nm for Cy-FN, and from 610 to 700 nm for Keto-Cy, $\lambda_{\text{ex}} = 730$ and 543 nm , respectively. Flow cytometric analysis: excitation wavelengths were 488 and 633 nm. The collected wavelengths were 610–670 nm and 750–810 nm, respectively.

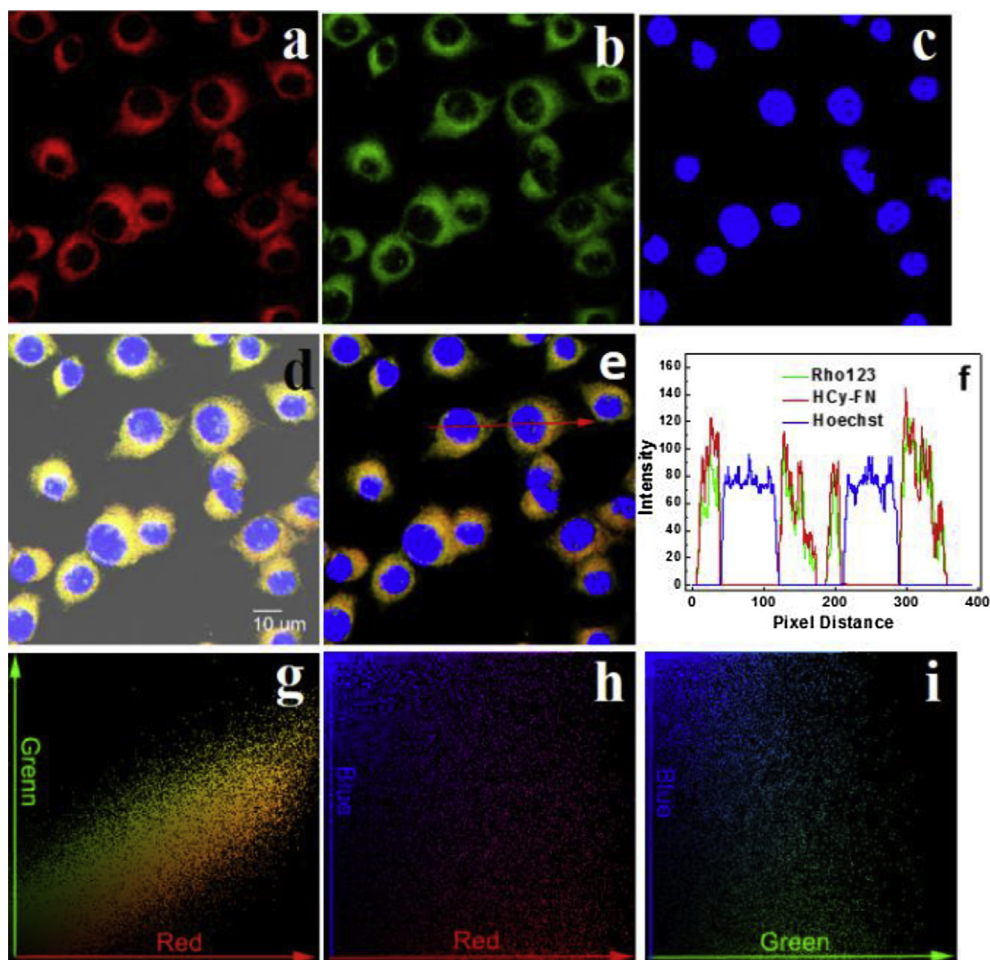


Fig. 3. Mitochondrial multicolor colocalization in RAW264.7 cells with probe HCY-FN, rhodamine 123, and Hoechst 33342. The cells were incubated with 1 μ M HCY-FN for 15 min (a), 1 μ g/mL rhodamine 123 for 15 min (b), and 1 μ g/mL Hoechst 33342 for 30 min (c). After washed with RPMI-1640, the cells were treated with PMA (10 nM) for 30 min. Fluorescence images collection windows: from 760 to 850 nm for (a), from 550 to 600 nm for (b), and from 440 to 500 nm for (c). $\lambda_{\text{ex}} = 730, 515, \text{ and } 405 \text{ nm}$, respectively. (d) Merged red, green, blue channels and bright field. (e) Merged red, green, and blue channels. (f) Intensity profile of regions of interest (red arrow in e) across two RAW264.7 cells. (g–i) Displayed the colocalization and correlation between two selected channels from (e): red, green and blue. (For interpretation of the references to colour in this figure legend, the reader is referred to the web version of this article.)

bioimaging. The dual-channel images were constructed via fluorescence collection windows: from 750 to 800 nm (channel 1) and from 610 to 700 nm (channel 2). In the control group, all the two cassette channels displayed faint fluorescence (Fig. 2 Row 1). After treated RAW264.7 cells with $\text{O}_2^{\cdot-}$, fluorescence collection channel 1 gave significant fluorescence enhancement as HCY-FN recovered its π -conjugate structure, while channel 2 still remained silent (Fig. 2 Row 2). The RAW264.7 cells in next group were first induced oxidative stress by incubated with $\text{O}_2^{\cdot-}$, and then exogenous H_2S was added to produce H_2S_n as RAW264.7 cells employed glutathione peroxidase (GPx) to regulate antioxidants and anti-inflammatory activities [59–62,64]. As might be expected, following lighted by $\text{O}_2^{\cdot-}$ in channel 1, the subsequent form of probe HCY-FN (that was Cy-FN) could respond to H_2S_n in channel 2 (Fig. 2 Row 3). As continued, the fluorescence of channel 1 quenched gradually, and the fluorescence of channel 2 increased steadily (Fig. 2 Row 4). We also tested that Cy-FN had no response to NaHS (Fig. S13). The mean fluorescence intensity of each condition shown in Fig. S12 was also quantified in histogram to allow for direct comparisons. We also performed flow cytometry assay to further confirm the fluorescence increase in living cells. As indicated in Fig. 2, the results which obtained from flow cytometry analysis were well consistent with those of confocal fluorescence microscopy. These results confirmed that HCY-FN was clearly

capable of monitoring H_2S_n formation in presence of $\text{O}_2^{\cdot-}$ in living cells. Furthermore, the probes HCY-FN, Cy-FN and Keto-Cy showed low cytotoxicity as determined via MTT assay. The result showed IC_{50} was 260, 300 and 230 μM for the three compounds, respectively.

3.5. Detection of $\text{O}_2^{\cdot-}$ and H_2S_n in mitochondria

Mitochondria are indispensable for energy production, which strangle the main thoroughfare for the survival of aerobic organisms. Mitochondria also hold both vital and pivotal functions in physiological and pathological issues [65]. Endogenous $\text{O}_2^{\cdot-}$ is inevitably induced by oxygen during electrons leak from respiratory chain [22]. The initial $\text{O}_2^{\cdot-}$ is often contributed to the immune system and redox signaling. There is evidence suggesting that cellular $\text{O}_2^{\cdot-}$ (the precursor of H_2O_2) burst can arouse H_2S production [66], which may further imply diverse redox-active events based on $\text{O}_2^{\cdot-}/\text{H}_2\text{S}$ crosstalk that links to H_2S_n formation in cells. We now attempted to check the ability of HCY-FN to monitor endogenous release of $\text{O}_2^{\cdot-}$ and H_2S_n in mitochondria in situ successively.

We obtained endogenous $\text{O}_2^{\cdot-}$ by way of utilizing phorbol 12-myristate 13-acetate (PMA) to induce respiratory burst in macrophages, followed by employing HCY-FN to detect mitochondrial

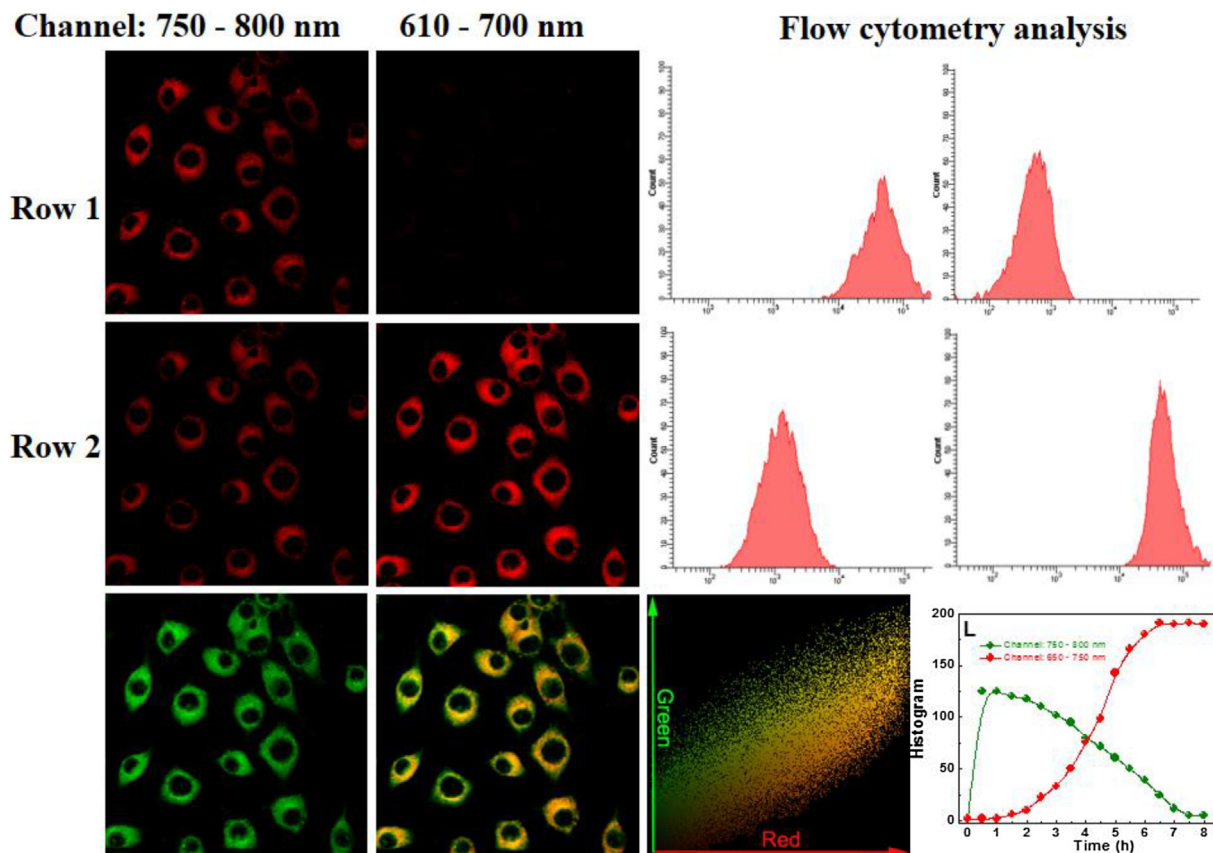


Fig. 4. Fluorescence confocal microscopic images of RAW264.7 cells loaded with 1 μM HCy-FN and exposed to endogenous $\text{O}_2^{\cdot-}$ and H_2S_n induced by PMA and LPS. The cells were incubated under 37 $^\circ\text{C}$ for 15 min in RPMI-1640 containing 1 μM HCy-FN. Then washed by RPMI-1640, the cells were next treated with PMA (10 nM) for 30 min. LPS (1 $\mu\text{g}/\text{ml}$) was added to induce CSE overexpression for promoting H_2S_n production. Fluorescence changes in two channels were observed during 6 h. The time dependent intensities of the images were presented as histogram. The colocalization with 1 $\mu\text{g}/\text{mL}$ rhodamine 123 suggested our probe functioned well in mitochondria. Fluorescence collection windows: from 760 to 850 nm for Cy-FN, from 610 to 700 nm for Keto-Cy, and from 550 to 600 nm for rhodamine 123, $\lambda_{\text{ex}} = 730, 543, \text{ and } 515 \text{ nm}$, respectively.

$\text{O}_2^{\cdot-}$ in real time. The multicolor colocalization method that based on the simultaneous acquisition and analysis of spectrally separated images can measure molecular distances with accuracy better than 10 nm [67]. Firstly, we employed the colocalization method to verify HCy-FN functioned in mitochondria. The costaining dyes were a mitochondria tracker rhodamine 123 and a DNA marker Hoechst 33342. RAW264.7 cells were loaded with 1 $\mu\text{g}/\text{mL}$ Hoechst 33342 for 30 min, 1 μM HCy-FN and 1 $\mu\text{g}/\text{mL}$ rhodamine 123 for 15 min. After washed with RPMI-1640, the cells were treated with PMA (10 nM) for 30 min to induce $\text{O}_2^{\cdot-}$ burst. The spectrally separated images acquired from the three dyes were estimated using Image-Pro Plus software (Fig. 3). The images of Cy-FN and rhodamine 123 (Fig. 3a and b) merged well (Fig. 3d and e). We obtained the Pearson's coefficient $R_r = 0.98$ and the Manders' coefficients $m_1 = 0.99, m_2 = 0.98$. The intensity profiles of the linear regions of interest across RAW264.7 cells costained with Cy-FN and rhodamine 123 (red arrow in Fig. 3e) were depicting a full synchrony (Fig. 3f). Hoechst 33342 offered a clear sublocation in the nucleus. Next we performed intensity correlation analysis of the dyads for parts a, b and c of Fig. 3. We counted the intensity of stain color-pair for each pixel to demonstrate the intensity distribution of the two colocalization dyes. As shown in Fig. 3g–i, only the costaining Cy-FN against rhodamine 123 illustrated a highly correlated plot. Flow cytometry analysis of mitochondrial isolation for the stimulated macrophages were also performed as secondary evidence of the fluorescent signal changes in mitochondria (Fig. S16). All of these results confirmed that our probe could specifically localize in mitochondria. And our probe also indicated a potentially

powerful approach for real-time imaging mitochondrial $\text{O}_2^{\cdot-}$ changes in cells.

We next investigated whether HCy-FN could measure mitochondrial H_2S_n levels derived from cystathionine γ -lyase (CSE) in presence of $\text{O}_2^{\cdot-}$, which might be a biosynthesis approach in cells. CSE is the major enzyme that catalyzes H_2S production in cells. Macrophages can overexpress the H_2S -forming enzyme when stimulated by lipopolysaccharide (LPS) [68]. The cells in Fig. 4 were incubated with 1 μM HCy-FN for 15 min under 37 $^\circ\text{C}$. After washed with RPMI-1640, the cells were treated with PMA (10 nM) for 30 min to induce the mitochondrial oxidative stress. As expected, channel 1 exhibited an increasing in fluorescence response due to the existence of $\text{O}_2^{\cdot-}$ (Fig. 4 Row 1). The same cells were next incubated with LPS (1 $\mu\text{g}/\text{mL}$) for 6 h to induce CSE mRNA and protein expression for promoting the initial H_2S production in RAW264.7 cells. Fluorescence images manifested evident changes in two collected channels as the probe next sensed H_2S_n (Fig. 4 Row 2). The time dependent intensities of the two channels were observed during 6 h and were presented as histogram (Fig. 4L). The colocalization with rhodamine 123 suggested our probe could detect H_2S_n in mitochondria. The cells were pretreated by the CSE inhibitor, DL-propargylglycine, giving much weaker fluorescence response in channel 2 (Fig. S18). Flow cytometry analysis and mitochondrial isolation for the stimulated macrophages were also performed to confirm the fluorescent signal changes (Fig. 4). Above results demonstrated that our probe could selectively multi-respond to the potential mitochondrial redox signaling process between $\text{O}_2^{\cdot-}$ and H_2S_n in real time and in situ.

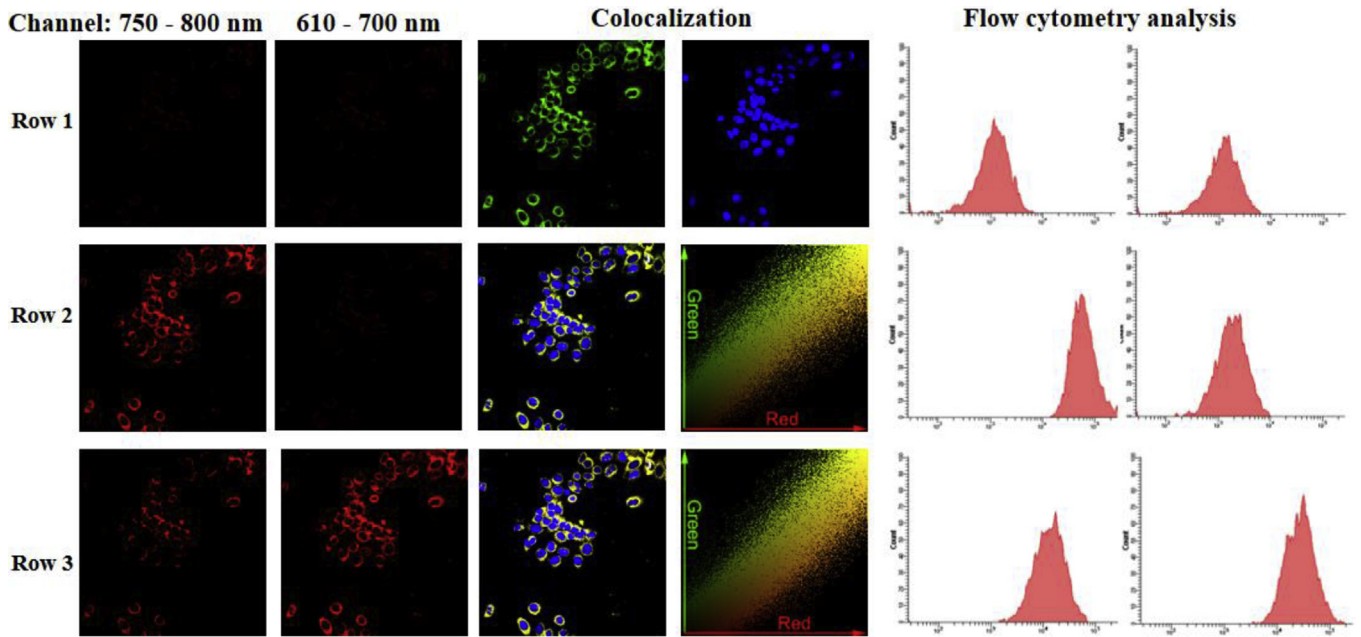


Fig. 5. Mitochondrial multicolor colocalization in RAW264.7 cells with probe HCy-FN, MitoTracker[®] Green FM, and Hoechst 33342. The cells were loaded with 1 μ M HCy-FN for 15 min, 1 μ g/mL MitoTracker[®] Green FM for 20 min, and 1 μ g/mL Hoechst 33342 for 30 min. After washed with RPMI-1640, the cells were treated with qaraquat (50 nM) for 30 min (Row 2). Washed the cells with RPMI-1640, LPS (1 μ g/ml) was added to induce CSE overexpression for promoting H_2S_n production. Fluorescence changes in two channels were observed during 6 h (Row 3). Fluorescence collection windows: from 760 to 850 nm for Cy-FN, from 610 to 700 nm for Keto-Cy, from 550 to 600 nm for rhodamine 123, and from 440 to 500 nm for Hoechst. λ_{ex} = 730, 543, 515, and 405 nm respectively. Merged red, green, blue channels displayed the colocalization and correlation between two selected channels. Flow cytometric analysis illustrated the corresponding fluorescence changes. The excitation wavelengths were 488 and 633 nm. The collected wavelengths were 610–670 nm and 750–810 nm, respectively. (For interpretation of the references to colour in this figure legend, the reader is referred to the web version of this article.)

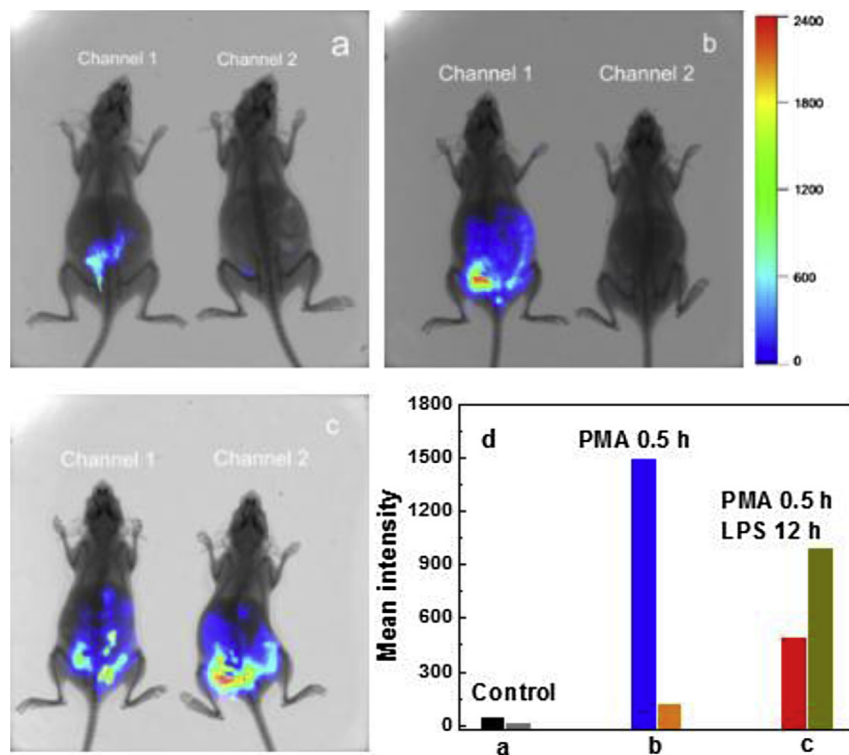


Fig. 6. In vivo imaging of O_2^- and H_2S_n in peritoneal cavity of the mice BALB/c. Images constructed from fluorescence collection window channel 1: 750–850 nm, λ_{ex} = 735 nm; channel 2: 600–700 nm, λ_{ex} = 530 nm. (a) HCy-FN (1 μ M, 50 μ L in 1:9 acetonitrile/saline v/v) was injected in the i.p. cavity for 0.5 h. (b) Mice were loaded with 1 μ M HCy-FN for 0.5 h, then injected i.p. with PMA (100 nM, 100 μ L in 1:9 acetonitrile/saline v/v) for 0.5 h. (c) Mice treated as (b) described, then injected i.p. with LPS (10 μ g/mL, 100 μ L in 1:9 acetonitrile/saline v/v) for 12 h. (d) Quantification of total photon flux from each mouse (a–c). The total number of photons from the entire peritoneal cavity of the mice (a–c) was integrated.

Despite the mechanism of $O_2^{\cdot-}$ burst induced by PMA is related to the disruption of mitochondrial respiration, the intraphagosomal production of $O_2^{\cdot-}$ can also be activated by protein kinase C agonists such as PMA. Additionally, $O_2^{\cdot-}$ can traverse both the plasma and mitochondrial membranes via anion channels to play cytoplasmic effects. This may cause obstruction for the source of $O_2^{\cdot-}$ in cells. Paraquat can stimulate $O_2^{\cdot-}$ production in nonactivated macrophages through disruption of the mitochondrial electron transport chain [69]. We next employed paraquat and LPS to elevate the levels of $O_2^{\cdot-}$ and H_2S_n in mitochondria. As illustrated in Fig. 5, the intensity analysis of stain color-pair displayed a highly correlated plot with the Pearson's coefficient $R_r = 0.97$ and the Manders' coefficients $m_1 = 0.98$, $m_2 = 0.98$. Flow cytometry analysis for the cells and the isolated mitochondria (Fig. S19) were also performed to confirm the fluorescent signal changes in cells and in mitochondria. All the results showed that the probe HCy-FN could specifically localize in mitochondria to detect $O_2^{\cdot-}$ and H_2S_n in real time and in situ.

3.6. Visualization of $O_2^{\cdot-}$ and H_2S_n in mice

With the consequence obtained from cell research in hand, we strongly suggested that our NIR probe would be favorable for the potential of being used to image $O_2^{\cdot-}$ and H_2S_n in vivo successively. We utilized BALB/c mice as biological models to assess this issue. The mice were injected into intraperitoneal (i.p.) cavity with our probe, and then the changes of fluorescence imaging were observed using an in vivo imaging system (Bruker). The mice in Fig. 6a injected into i.p. cavity with HCy-FN (1 μ M, 50 μ L in 1:9 acetonitrile/saline v/v) displayed low signal intensity in two channels. Another group mice were loaded with 1 μ M HCy-FN for 0.5 h, then the mice were injected i.p. with PMA (100 nM, 100 μ L in 1:9 acetonitrile/saline v/v) for 0.5 h. Channel 1 emanated strong fluorescence from inside of the mice body (Fig. 6b) as the probe had detected $O_2^{\cdot-}$. Moreover, when the mice were then treated with LPS (10 μ g/mL, 100 μ L in 1:9 acetonitrile/saline v/v) for the next 12 h, a dramatically decreasing intensity fluorescence image in Channel 1, and a notable increasing fluorescence image was observed in Channel 2 (Fig. 6c), which implied the production of H_2S_n in presence of $O_2^{\cdot-}$. Fig. 6d listed the quantification of mean fluorescence intensity for each condition shown in parts a–c of Fig. 6. These results indicated that probe HCy-FN could be employed to directly detect $O_2^{\cdot-}$ and H_2S_n successively in living animals, which revealed the latent advantage of the new multi-response near-infrared fluorescent probe.

4. Conclusions

In summary, we develop a multiresponse near-infrared fluorescent probe for the detection of $O_2^{\cdot-}$ and H_2S_n successively with dual fluorescence response channel. We confirmed that H_2S_n can be derived from H_2S in the presence of $O_2^{\cdot-}$, which is considered to be a potential direct biosynthetic pathway for H_2S_n in cells. The mitochondria-targeting probe also exhibits highly selective response to $O_2^{\cdot-}$ and H_2S_n against other biological ROS and reactive sulfur species interferants. Fluorescence confocal microscopic imaging for the RAW264.7 cells illustrated that our probe can be used to investigate the process of $O_2^{\cdot-}$ burst and H_2S_n production in situ and in real-time. Flow cytometry analysis for cell experiments further confirm the bioimaging results. Finally, we successfully apply the probe to detect $O_2^{\cdot-}$ and H_2S_n in mice. The results of our efforts highlight that the multiresponse probe can be used as a direct chemical tool for the detection of $O_2^{\cdot-}$ and H_2S_n in cells and in mice.

Acknowledgments

We thank National Nature Science Foundation of China (NSFC) (No. 21405172, No. 21275158), the Innovation Projects of the CAS (Grant KZCX2-EW-206), the Strategic Priority Research Program of the Chinese Academy of Sciences (XDA11020702) and the program of Youth Innovation Promotion Association, CAS (Grant 2015170).

Appendix A. Supplementary data

Supplementary data related to this article can be found at <http://dx.doi.org/10.1016/j.biomaterials.2015.06.007>.

References

- [1] X. Chen, Y. Zhou, X. Peng, J. Yoon, Fluorescent and colorimetric probes for detection of thiols, *Chem. Soc. Rev.* 39 (2010) 2120–2135.
- [2] X. Li, X. Gao, W. Shi, H. Ma, Design strategies for water-soluble small molecular chromogenic and fluorogenic probes, *Chem. Rev.* 114 (2014) 590–659.
- [3] C.E. Paulsen, K.S. Carroll, Cysteine-mediated redox signaling: chemistry, biology, and tools for discovery, *Chem. Rev.* 113 (2013) 4633–4679.
- [4] Y. Yang, Q. Zhao, W. Feng, F. Li, Luminescent chemodosimeters for bioimaging, *Chem. Rev.* 113 (2013) 192–270.
- [5] J. Fan, M. Hu, P. Zhan, X. Peng, Energy transfer cassettes based on organic fluorophores: construction and applications in ratiometric sensing, *Chem. Soc. Rev.* 42 (2013) 29–43.
- [6] R. Wang, C. Yu, F. Yu, L. Chen, C. Yu, Molecular fluorescent probes for monitoring pH changes in living cells, *Trends Anal. Chem.* 29 (2010) 1004–1013.
- [7] F. Yu, X. Han, L. Chen, Fluorescent probes for hydrogen sulfide detection and bioimaging, *Chem. Commun.* 50 (2014) 12234–12249.
- [8] V.S. Lin, C.J. Chang, Fluorescent probes for sensing and imaging biological hydrogen sulfide, *Curr. Opin. Chem. Biol.* 16 (2012) 595–601.
- [9] G. Yang, L. Wu, B. Jiang, W. Yang, J. Qi, K. Cao, Q. Meng, A.K. Mustafa, W. Mu, S. Zhang, S.H. Snyder, R. Wang, H_2S as a physiologic vasorelaxant: hypertension in mice with deletion of cystathionine gamma-lyase, *Science* 322 (2008) 587–590.
- [10] B.D. Paul, S.H. Snyder, H_2S signalling through protein sulphydration and beyond, *Nat. Rev. Mol. Cell. Biol.* 13 (2012) 499–507.
- [11] L. Li, P. Rose, P.K. Moore, Hydrogen sulfide and cell signaling, *Annu. Rev. Pharmacol.* 51 (2011) 169–187.
- [12] R. Wang, Physiological implications of hydrogen sulfide: a whiff exploration that blossomed, *Physiol. Rev.* 92 (2012) 791–896.
- [13] V. Vitvitsky, O. Kabil, R. Banerjee, High turnover rates for hydrogen sulfide allow for rapid regulation of its tissue concentrations, *Antioxid. Redox Signal* 17 (2012) 22–31.
- [14] R. Greiner, Z. Pálinkás, K. Bäsell, D. Becher, H. Antelmann, P. Nagy, T.P. Dick, Polysulfides link H_2S to protein thiol oxidation, *Antioxid. Redox Signal* 19 (2013) 1749–1765.
- [15] J.I. Toohey, Sulfur signaling: is the agent sulfide or sulfane? *Anal. Biochem.* 413 (2011) 1–7.
- [16] N. Shibuya, M. Tanaka, M. Yoshida, Y. Ogasawara, T. Togawa, K. Ishii, H. Kimura, 3-Mercaptopyruvate sulfurtransferase produces hydrogen sulfide and bound sulfane sulfur in the brain, *Antioxid. Redox Signal* 11 (2009) 703–714.
- [17] P. Nagy, C.C. Winterbourn, Rapid reaction of hydrogen sulfide with the neutrophil oxidant hypochlorous acid to generate polysulfides, *Chem. Res. Toxicol.* 23 (2010) 1541–1543.
- [18] B.L. Predmore, D.J. Lefer, G. Gojon, Hydrogen sulfide in biochemistry and medicine, *Antioxid. Redox Signal* 17 (2012) 119–140.
- [19] T. Chatterji, K. Keerthi, K.S. Gates, Generation of reactive oxygen species by a persulfide (BnSSH), *Bioorg. Med. Chem. Lett.* 15 (2005) 3921–3924.
- [20] T. Ida, T. Sawa, H. Ihara, Y. Tsuchiya, Y. Watanabe, Y. Kumagai, M. Suematsu, H. Motohashi, S. Fujii, T. Matsunaga, M. Yamamoto, K. Ono, N.O. Devarie-Baez, M. Xian, J.M. Fukuto, T. Akaike, Reactive cysteine persulfides and S-polythiolation regulate oxidative stress and redox signaling, *Proc. Natl. Acad. Sci.* 111 (2014) 7606–7611.
- [21] T.S. Bailey, L.N. Zakharov, M.D. Pluth, Understanding hydrogen sulfide storage: probing conditions for sulfide release from hydrodisulfides, *J. Am. Chem. Soc.* 136 (2014) 10573–10576.
- [22] B. Halliwell, J.M.C. Gutteridge, *Free Radicals in Biology and Medicine*, Oxford University Press, Oxford, UK, 1999.
- [23] M. Iciek, L. Wiodek, Biosynthesis and biological properties of compounds containing highly reactive, reduced sulfane sulfur, *Pol. J. Pharmacol.* 53 (2001) 215–225.
- [24] X. Chen, X. Tian, I. Shin, J. Yoon, Fluorescent and luminescent probes for detection of reactive oxygen and nitrogen species, *Chem. Soc. Rev.* 40 (2011) 4783–4804.
- [25] P. Li, W. Zhang, K. Li, X. Liu, H. Xiao, W. Zhang, B. Tang, Mitochondria-targeted reaction-based two-photon fluorescent probe for imaging of superoxide anion in live cells and in vivo, *Anal. Chem.* 85 (2013) 9877–9881.

- [26] D.P. Murale, H. Kim, W.S. Choi, D.G. Churchill, Highly selective excited state intramolecular proton transfer (ESIPT)-based superoxide probing, *Org. Lett.* 15 (2013) 3946–3949.
- [27] K.M. Robinson, M.S. Janes, M. Pehar, J.S. Monette, M.F. Ross, T.M. Hagen, M.P. Murphy, J.S. Beckman, Selective fluorescent imaging of superoxide in vivo using ethidium-based probes, *Proc. Natl. Acad. Sci.* 103 (2006) 15038–15043.
- [28] C. Liu, W. Chen, W. Shi, B. Peng, Y. Zhao, H. Ma, M. Xian, Rational design and bioimaging applications of highly selective fluorescence probes for hydrogen polysulfides, *J. Am. Chem. Soc.* 136 (2014) 7257–7260.
- [29] W. Chen, C. Liu, B. Peng, Y. Zhao, A. Pacheco, M. Xian, New fluorescent probes for sulfane sulfurs and the application in bioimaging, *Chem. Sci.* 4 (2013) 2892–2896.
- [30] M. Gao, F. Yu, H. Chen, L. Chen, Near-infrared fluorescent probe for imaging mitochondrial hydrogen polysulfides in living cells and in vivo, *Anal. Chem.* 87 (2015) 3631–3638.
- [31] M. Gao, R. Wang, F. Yu, J. You, L. Chen, A near-infrared fluorescent probe for the detection of hydrogen polysulfides biosynthetic pathways in living cells and in vivo, *Analyst* 140 (2015) 3766–3772.
- [32] L. Zeng, S. Chen, T. Xia, W. Hu, C. Li, Z. Liu, Two-photon fluorescent probe for detection of exogenous and endogenous hydrogen persulfide and polysulfide in living organisms, *Anal. Chem.* 87 (2015) 3004–3010.
- [33] F. Yu, P. Li, B. Wang, K. Han, Reversible near-infrared fluorescent probe introducing tellurium to mimetic glutathione peroxidase for monitoring the redox cycles between peroxynitrite and glutathione in vivo, *J. Am. Chem. Soc.* 135 (2013) 7674–7680.
- [34] F. Yu, P. Li, G. Li, G. Zhao, T. Chu, K. Han, A near-IR reversible fluorescent probe modulated by selenium for monitoring peroxynitrite and imaging in living cells, *J. Am. Chem. Soc.* 133 (2011) 11030–11033.
- [35] F. Yu, P. Li, P. Song, B. Wang, J. Zhao, K. Han, Facilitative functionalization of cyanine dye by an on-off-on fluorescent switch for imaging of H₂O₂ oxidative stress and thiols reducing repair in cells and tissues, *Chem. Commun.* 48 (2012) 4980–4982.
- [36] F. Yu, P. Song, P. Li, B. Wang, K. Han, Development of reversible fluorescence probes based on redox oxoammonium cation for hypobromous acid detection in living cells, *Chem. Commun.* 48 (2012) 7735–7737.
- [37] Q. Zhang, Z. Zhu, Y. Zheng, J. Cheng, N. Zhang, Y.T. Long, J. Zheng, X. Qian, Y. Yang, A three-channel fluorescent probe that distinguishes peroxynitrite from hypochlorite, *J. Am. Chem. Soc.* 134 (2012) 18479–18482.
- [38] S. Takahashi, W. Piao, Y. Matsumura, T. Komatsu, T. Ueno, T. Terai, T. Kamachi, M. Kohno, T. Nagano, K. Hanaoka, Reversible off-on fluorescence probe for hypoxia and imaging of hypoxia-normoxia cycles in live cells, *J. Am. Chem. Soc.* 134 (2012) 19588–19591.
- [39] T. Egawa, K. Hirabayashi, Y. Koide, C. Kobayashi, N. Takahashi, T. Mineno, T. Terai, T. Ueno, T. Komatsu, Y. Ikegaya, N. Matsuki, T. Nagano, K. Hanaoka, Red fluorescent probe for monitoring the dynamics of cytoplasmic calcium ions, *Angew. Chem. Int. Ed.* 52 (2013) 3874–3877.
- [40] A.T. Wrobel, T.C. Johnstone, L.A. Deliz, S.J. Lippard, P. Rivera-Fuentes, A fast and selective near-infrared fluorescent sensor for multicolor imaging of biological nitroxyl (HNO), *J. Am. Chem. Soc.* 136 (2014) 4697–4705.
- [41] W. Lin, D. Buccella, S.J. Lippard, Visualization of peroxynitrite-induced changes of labile Zn²⁺ in the endoplasmic reticulum with benzoresorufin-based fluorescent probes, *J. Am. Chem. Soc.* 135 (2013) 13512–13520.
- [42] J. Liu, Y. Sun, Y. Huo, H. Zhang, L. Wang, P. Zhang, D. Song, Y. Shi, W. Guo, Simultaneous fluorescence sensing of Cys and GSH from different emission channels, *J. Am. Chem. Soc.* 136 (2014) 574–577.
- [43] J. Liu, Y. Sun, J. Liu, H. Zhang, Y. Huo, Y. Shi, W. Guo, Simultaneous fluorescent imaging of Cys/Hcy and GSH from different emission channels, *Chem. Sci.* 5 (2014) 3183–3188.
- [44] X. Yang, Q. Huang, Y. Zhong, Z. Li, H. Li, M. Lowry, J.O. Escobedo, R.M. Strongin, A dual emission fluorescent probe enables simultaneous detection of glutathione and cysteine/homocysteine, *Chem. Sci.* 5 (2014) 2177–2183.
- [45] Q. Xu, K.A. Lee, S. Lee, K.M. Lee, W.J. Lee, J. Yoon, A highly specific fluorescent probe for hypochlorous acid and its application in imaging microbe-induced HOCl production, *J. Am. Chem. Soc.* 135 (2013) 9944–9949.
- [46] Y. Li, H. Wang, J. Li, J. Zheng, X. Xu, R. Yang, Simultaneous intracellular β -D-glucosidase and phosphodiesterase I activities measurements based on a triple-signaling fluorescent probe, *Anal. Chem.* 83 (2011) 1268–1274.
- [47] H. Kobayashi, Y. Koyama, T. Barrett, Y. Hama, C.A.S. Regino, I.S. Shin, B.S. Jang, N. Le, C.H. Paik, P.L. Choyke, Y. Urano, Multimodal nanoprobe for radionuclide and five-color near-infrared optical lymphatic imaging, *ACS Nano* 1 (2007) 258–264.
- [48] Y. Li, H. Wang, J. Li, J. Zheng, X. Xu, R. Yang, Simultaneous intracellular β -D-glucosidase and phosphodiesterase I activities measurements based on a triple-signaling fluorescent probe, *Anal. Chem.* 83 (2011) 1268–1274.
- [49] L. Strekowski, M. Lipowska, G. Patonay, Facile derivatizations of heptamethine cyanine dyes, *Synth. Commun.* 23 (1992) 2593–2598.
- [50] K. Kundu, S.F. Knight, N. Willett, S. Lee, W.R. Taylor, N. Murthy, Hydrocyanines: a class of fluorescent sensors that can image reactive oxygen species in cell culture, tissue, and in vivo, *Angew. Chem. Int. Ed.* 48 (2009) 299–303.
- [51] C.P. LeBel, H. Ischiropoulos, S.C. Bondy, Evaluation of the probe 2',7'-dichlorofluorescein as an indicator of reactive oxygen species formation and oxidative stress, *Chem. Res. Toxicol.* 5 (1992) 227–231.
- [52] S.E. Buxser, G. Sawada, T.J. Raub, Analytical and numerical techniques for evaluation of free radical damage in cultured cells using imaging cytometry and fluorescent indicators, *Methods Enzymol.* 300 (1999) 256–275.
- [53] V. Marx, Probes: seeing in the near infrared, *Nat. Methods* 11 (2014) 717–720.
- [54] L. Yuan, W. Lin, K. Zheng, L. He, W. Huang, Far-red to near infrared analyte-responsive fluorescent probes based on organic fluorophore platforms for fluorescence imaging, *Chem. Soc. Rev.* 42 (2013) 622–661.
- [55] Y. Kimura, Y. Mikami, K. Osumi, M. Tsugane, J. Oka, H. Kimura, Polysulfides are possible H₂S-derived signaling molecules in rat brain, *FASEB J.* 27 (2013) 2451–2457.
- [56] K.M. Miranda, D.A. Wink, Persulfides and the cellular thiol landscape, *Proc. Natl. Acad. Sci.* 111 (2014) 7505–7506.
- [57] Z. Guo, G.H. Kim, I. Shin, J. Yoon, A cyanine-based fluorescent sensor for detecting endogenous zinc ions in live cells and organisms, *Biomaterials* 33 (2012) 7818–7827.
- [58] Z. Guo, S.W. Nam, S. Park, J. Yoon, A highly selective ratiometric near-infrared fluorescent cyanine sensor for cysteine with remarkable shift and its application in bioimaging, *Chem. Sci.* 3 (2012) 2760–2765.
- [59] M. Lu, L.F. Hu, G. Hu, J.S. Bian, Hydrogen sulfide protects astrocytes against H₂O₂-induced neural injury via enhancing glutamate uptake, *Free Radic. Biol. Med.* 45 (2008) 1705–1713.
- [60] L. Li, H. Xin, H. Qi, B. He, Z. Yi, Role of cystathionine γ -lyase/hydrogen sulfide pathway in cardiovascular disease: a novel therapeutic strategy? *Antioxid. Redox Signal* 17 (2012) 106–118.
- [61] Y. Ju, W. Zhang, Y. Pei, G. Yang, H₂S signaling in redox regulation of cellular functions, *Can. J. Physiol. Pharmacol.* 91 (2013) 8–14.
- [62] Y. Wen, H. Wang, S.H. Kho, S. Rinkiko, X. Sheng, H. Shen, Y. Zhu, Hydrogen sulfide protects HUVECs against hydrogen peroxide induced mitochondrial dysfunction and oxidative stress, *PLoS One* 8 (2013) e53147.
- [63] C.C. Winterbourn, Reconciling the chemistry and biology of reactive oxygen species, *Nat. Chem. Biol.* 4 (2008) 278–286.
- [64] W.J. Jung, M.K. Sung, Effects of major dietary antioxidants on inflammatory markers of RAW 264.7 macrophages, *Biofactors* 21 (2004) 113–117.
- [65] S. Fulda, L. Galluzzi, G. Kroemer, Targeting mitochondria for cancer therapy, *Nat. Rev. Drug Discov.* 9 (2010) 447–464.
- [66] V.S. Lin, A.R. Lippert, C.J. Chang, Cell-trappable fluorescent probes for endogenous hydrogen sulfide signaling and imaging H₂O₂-dependent H₂S production, *Proc. Natl. Acad. Sci.* 110 (2013) 7131–7135.
- [67] X. Michalet, T.D. Lacoste, S. Weiss, Ultrahigh-resolution colocalization of spectrally separable point-like fluorescent probes, *Methods* 25 (2001) 87–102.
- [68] X. Zhu, S. Liu, Y. Liu, S. Wang, X. Ni, Glucocorticoids suppress cystathionine gamma-lyase expression and H₂S production in lipopolysaccharide-treated macrophages, *Cell. Mol. Life Sci.* 67 (2010) 1119–1132.
- [69] G.C. Van de Bittner, E.A. Dubikovskaya, C.R. Bertozzi, C.J. Chang, In vivo imaging of hydrogen peroxide production in a murine tumor model with a chemoselective bioluminescent reporter, *Proc. Natl. Acad. Sci. U. S. A.* 107 (2010) 21316–21321.